Mon. Not. R. Astron. Soc. **000**, 1–8 (2005) Printed 5 February 2008 (MN LATEX style file v2.2)

The Influence of Large–Scale Structure on Halo Shapes and Alignments

Gabriel Altay[1⋆], Jörg M. Colberg[1,2] and Rupert A.C. Croft[1]
[1] *Carnegie Mellon University, Department of Physics, 5000 Forbes Ave, Pittsburgh, PA 15213, USA*
[2] *University of Pittsburgh, Department of Physics and Astronomy, 3941 O'Hara Street, Pittsburgh PA 15260, USA*

5 February 2008

ABSTRACT
Alignments of galaxy clusters (the Binggeli effect), as well as of galaxies themselves have long been studied both observationally and theoretically. Here we test the influence of large-scales structures and tidal fields on the shapes and alignments of cluster–size and galaxy–size dark matter halos. We use a high–resolution N–body simulation of a ΛCDM universe, together with the results of Colberg et al. (2005), who identified filaments connecting pairs of clusters. We find that cluster pairs connected by a filament are strongly aligned with the cluster-cluster axis, whereas unconnected ones are not. For smaller, galaxy–size halos, there also is an alignment signal, but its strength is independent of whether the halo is part of an obvious large–scale structure. Additionally, we find no measureable dependence of galaxy halo shape on membership of a filament. We also quantify the influence of tidal fields and find that these do correlate strongly with alignments of halos. The alignments of most halos are thus caused by tidal fields, with cluster–size halos being strongly aligned through the added mechanism of infall of matter from filaments.

Key words: Cosmology: observations – large-scale structure of Universe

1 INTRODUCTION

Galaxy redshift surveys such as the 2dFGRS (Colless et al. 2001) or the Sloan Digital Sky Survey (York et al. 2000) and N–body simulations of cosmic structure formation (for example Springel et al. 2005 and references therein) demonstrate the existence of a complicated network of matter. At the most prominent positions in this network, massive clusters of galaxies can be found, which are interconnected by filaments and, to a lesser degree, sheets. In both observations and simulations clusters are aspherical systems, a fact which has lead to investigations of the degree and origin of asphericity and of possible alignments between neighbouring objects. In this paper we use an N–body simulation of a ΛCDM universe to study the link between this network of structure and the shapes and alignments of galaxies and clusters.

Binggeli (1982) first investigated the alignment of galaxy clusters, finding that for the 44 Abell clusters in a sample there was a strong longitudinal alignment signal (clusters tend to point towards each other, the "Binggeli effect"). This was seen for cluster-cluster separations of up to $\sim 15\ h^{-1}$ Mpc[1]. Most follow–up studies, optical and otherwise, have confirmed Binggeli's results (Flin 1987, Rhee & Katgert 1987, West 1989, Rhee et al. 1992, Plionis 1994, West et al. 1995, Chambers et al. 2000 and 2002), although there were also some negative reports (Struble & Peebles 1985, Ulmer et al. 1989).

On the theoretical side, much attention has been devoted to the shapes of dark matter halos (for example, the radial density profile was examined by Navarro et al. 1997, Moore et al. 1999, and the asphericity of galaxies and/or clusters by Jing & Suto 2002, Bailin & Steinmetz 2004, Hopkins et al. 2004, Kasun & Evrard 2004, Allgood et al. 2005, Lee et al. 2005b, and Paz et al. 2005). The alignments of halos have been getting somewhat less attention. Splinter et al. (1997), Onuora & Thomas (2000), and Faltenbacher et al. (2002) have all found significant alignments of galaxy cluster halos, as did Kasun & Evrard (2004), Hopkins et al. (2005), and Basilakos et al. (2005). Galaxy–sized halos also have a strong tendency to be aligned in the same direction as other nearby halos (see e.g. Heavens, Refregier & Heymans 2000, Croft & Metzler 2000), as well as pointing along the direction vector to nearby halos (e.g., Li & Croft 2005). This

⋆ E-mail: galtay@andrew.cmu.edu

[1] Throughout this work, we express the Hubble constant as $H_0 = 100\,h$ km/sec/Mpc.

latter signal, the intrinsic density–shear correlation has been recently seen in observational galaxy data by Mandelbaum et al. (2005), and Agustsson & Brainerd (2005).

It is not immediately obvious what causes the alignment of halos. As shown in Van Haarlem & Van de Weygaert (1993), clusters tend to orient themselves toward the direction of the last matter infall (as shown in Colberg et al. 1999, matter falls into cluster predominantly from filaments). But there is also a positive correlation between the inertia tensor of a cluster and its surrounding tidal field (Bond et al. 1996; as shown in Lee et al. 2005b, the axis–ratio distribution of halos can be modelled analytically on the basis of this, also see Lee et al. 2005a). In reality, both effects will probably be intertwined.

Hopkins et al. (2005) attempt to connect the alignment between cluster pairs and large–scale structure by looking at the number density of clusters contained in a cylinder that connects the two clusters. They find that as the number density rises, so does the average cluster alignment. While this indicates that filaments between clusters might cause increased alignment, for a more general analysis it is necessary to investigate cluster samples for which the inter-cluster filaments are found with reference to the density field itself. Such a set of filaments would also make possible an investigation of shapes and alignments of halos much smaller than galaxy clusters.

Colberg et al. (2005) investigated inter–cluster configurations of matter in a high–resolution simulation of cosmic structure and found a complete set of filaments. Here we will use their data as the basis for a detailed investigation of the connection between large–scale structure and halo alignments. In particular, we will investigate whether there is a connection between the alignment of pairs of clusters and the existence (or non–existence) of a filament between them. We will also study whether halos of mass smaller than that of a massive cluster are aligned with filaments and/or the tidal fields of the clusters. The latter is interesting in the light of an algorithm proposed by Pimbblet (2005) to locate filaments in galaxy redshift catalogues.

This work is organized as follows. In Section 2 we describe the simulation, in Section 3 we study the alignments of halos between pairs of clusters connected by filaments or with voids in between them, and in Section 4, we briefly re–visit ellipticities of halos. Section 5 contains a summary and discussion.

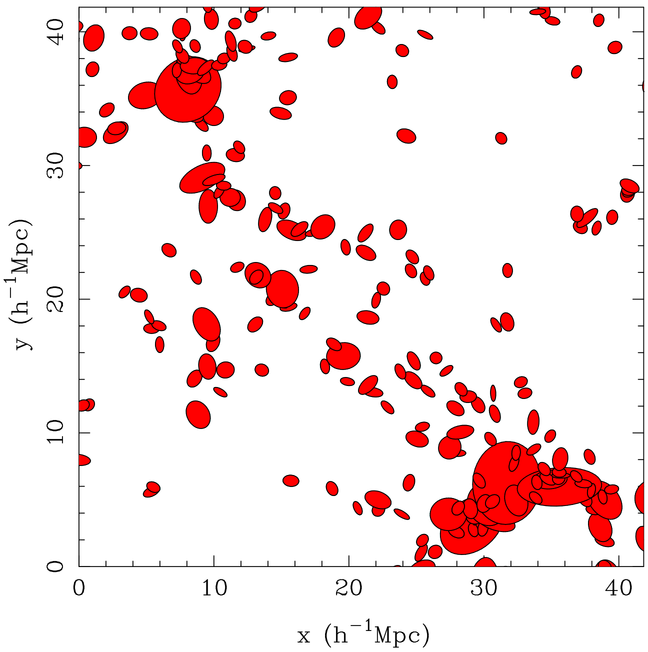

Figure 1. A part of a thin slice of thickness $15\,h^{-1}$ Mpc through the simulation volume, showing all halos as ellipsoids. The ellipsoids are scaled according to their mass, and their orientations correspond to those of the halo mass distributions. The plot is centered on one of the filaments found by Colberg et al. (2005), which spans two clusters, in the top left and bottom right hand corners of the panel.

2 THE SIMULATION

We make use of the high–resolution ΛCDM simulation introduced in Jenkins et al. (1998). The simulation parameters ($\Omega = 0.3$, $\Lambda = 0.7$, $h = 0.7$, and $\sigma_8 = 0.9$) are in good agreement with the currently accepted standard cosmology (Colless et al. 2001, Spergel et al. 2003, Seljak et al. 2005). The simulation follows the evolution of 256^3 Dark Matter particles in a cubical volume of size $(141.3\,h^{-1}\,\mathrm{Mpc})^3$ on a side, resulting in a particle mass of $1.4 \cdot 10^{10}\,h^{-1}\,M_\odot$.

2.1 The Halo Catalog

The group catalogue is obtained by running a standard friends–of–friends group finder on the full particle set, using a linking length of $b = 0.2$ times the mean interparticle separation. We use all groups with 50 particles or more for the analysis, which results in a total sample of 17461 halos. Our choice of the minimum halo mass is motivated by the fact that for less than 50 particles, the structure of a halo cannot be reliably determined (see e.g. the tests in Kasun & Evrard 2004). In the following, we will refer to the 170 most massive groups as clusters and to all others as halos. The cluster sample was designed to match the space density of Abell clusters as outlined in Colberg et al. (2005).

For each halo, we compute its principal axes by diagonalizing the moment of inertia tensor

$$I_{ij} = \sum x_i x_j \, , \tag{1}$$

where the sum is over all particles in the halo, and the coordinates are defined with respect to the center of mass of the group. The resulting eigenvalues a, b, and c are sorted by size, in descending order. The ellipticity of a group is then defined by

$$\epsilon = 1 - \sqrt{c/a} \, . \tag{2}$$

2.2 Filament Finding

We make use of the filament catalogue described by Colberg et al. (2005). In that paper, intercluster filaments were found by investigating the configuration of matter between neighbouring clusters. The mass distributions between all pairs of clusters (up to the 12th nearest neighbour of each cluster) were projected onto orthogonal planes. The results were then visually classified according to the appearance of

the projections (essentially into either a filament, absence of a structure, or rarely, a sheet). We will use the Colberg et al. (2005) classifications to examine alignments of halos and clusters with the cluster–cluster axes, and how it depends on the presence of a filaments..

Figure 1 shows a small piece of the simulation volume, with halos being plotted as ellipsoids. The ellipsoids are scaled according to their mass, and the orientations of the ellipsoids correspond to those of the actual mass distributions. The region shown in the plot encompasses a pair of clusters connected by a filament. The same filament is shown bottom–center in Figure 1 of Colberg et al. (2005). The filament is clearly visible, although any coherent alignments of the halos is difficult to pick out by eye. We will examine this statistically in the next section.

3 ALIGNMENTS OF HALOS

3.1 Halo Alignments in Filaments

For each cluster pair, we examine the halos that lie in the cylinder whose central axis is defined by the cluster–cluster axis and whose radius extends $70\,h^{-1}$ Mpc from the cluster–cluster axis. By going out to these large radii we cover as much of the simulation volume for each cluster pair as possible. We define two vectors $\hat{\mathbf{u}}_1$ and $\hat{\mathbf{u}}_2$ such that $\hat{\mathbf{u}}_1$ lies on the cluster–cluster axis, and $\hat{\mathbf{u}}_2$ points along one of the halo principal axes. Our measure of the alignment between them is defined by

$$|cos(\phi)| = |\hat{\mathbf{u}}_1 \cdot \hat{\mathbf{u}}_2| \tag{3}$$

where ϕ is the angle between the two vectors. For each of the three eigenaxes we compute this alignment.

3.1.1 Filament–Halo Alignments

In Figure 2, we plot the alignments of the principal axes of the halos with the cluster–cluster axis as a function of the perpendicular distance from that axis. The rows show the major, intermediate, and minor axes. In the leftmost, center, and rightmost columns we plot alignments of halos, of halos plus clusters, and of clusters, respectively. Cluster pairs which are connected by a filament are shown using squares, whereas asterisks are used for cluster pairs for which no coherent structure was found along the cluster–cluster axis. Errors bars are computed assuming Poissonian statistics. The dotted line shows the expectation for a random sample with no alignments.

For small separations from the cluster–cluster axis, the major and minor axes of halos are aligned and anti–aligned with that axis, respectively (leftmost column of Figure 2). Interestingly, there is no clear difference between those cluster pairs that are connected by a filament and those that are not connected at all. For galaxy–size halos therefore the fact that they lie in a filament or not does not affect their alignments (we will examine the effect on their ellipticities in Section 4.2).

The alignment signals become small at larger separations from the cluster–cluster axis. At separations of around $4\,h^{-1}$ Mpc the alignment signal is almost absent. As can be seen from Figure 8 in Colberg et al. (2005), at this scale, the averaged density profile of filaments has dropped strongly from its central value. However, given that we do not find a difference in the alignments between connected and unconnected cluster pairs, this finding has to be treated as a mere coincidence.

We note that the (anti) alignment signal is somewhat stronger for the minor axes than for major axes. Also, for the minor axes, there is a small difference between halos in filaments and halos elsewhere, although the error bars are relatively large. The intermediate halo axes are neither aligned nor anti–aligned with the cluster–cluster axes.

3.1.2 Filament–Cluster Alignments

The rightmost column of Figure 2 shows the alignment results for clusters. The major and minor axes of the clusters connected by filaments are aligned and anti–aligned with those filaments, respectively. Although the statistical uncertainty is quite large, the signal is significantly stronger than for galaxy–size halos. However, no such signal exists for cluster pairs that are not connected by filaments, which again is very different from the galaxy halo result. This finding provides an explanation for the Bingelli effect, which is directly connected to the presence of filaments.

3.2 Alignments as a Function of Projected Distance from the Cluster–Cluster Axis

Having examined alignments as a function of the radial distance from cluster–cluster axes, we now turn our attention to the dependence of any alignment signal on the distance of a halo from its nearest cluster, i.e. along the cluster–cluster axis. We restrict this analysis to all halos that are within $1.5\,h^{-1}$ Mpc from the axis.

Figure 3 shows the alignments for the three halo axes, both for halos (top row) and for halos plus clusters (bottom row). The symbols are the same as in Figure 2. We scale the halo–cluster separations on the x–axis such that a halo position just outside the virial radius of the nearest cluster is at position 0, whereas a halo right in the center between both clusters sits is at position 1. L is the total length of a cluster–cluster axis, and $d_{\rm proj}$ corresponds to the distance of a halo from the nearer one of the clusters that define the cluster–cluster axis. As before, the dotted line shows the expectation for a random sample with no alignments.

Figure 3 shows that the magnitude of the alignments does not depend on the distance of a halo from the nearest cluster. There also is no difference between cluster pairs that are connected by a filament and those that intersect a void.

3.3 Alignments as a Function of Cluster–Cluster Tidal Fields

The presence of tidal fields can provide a very natural explanation for the alignments and shapes of objects. In the following sections, we will study the influence of the tidal forces exterted by the clusters that are used to define the cluster–cluster configurations.

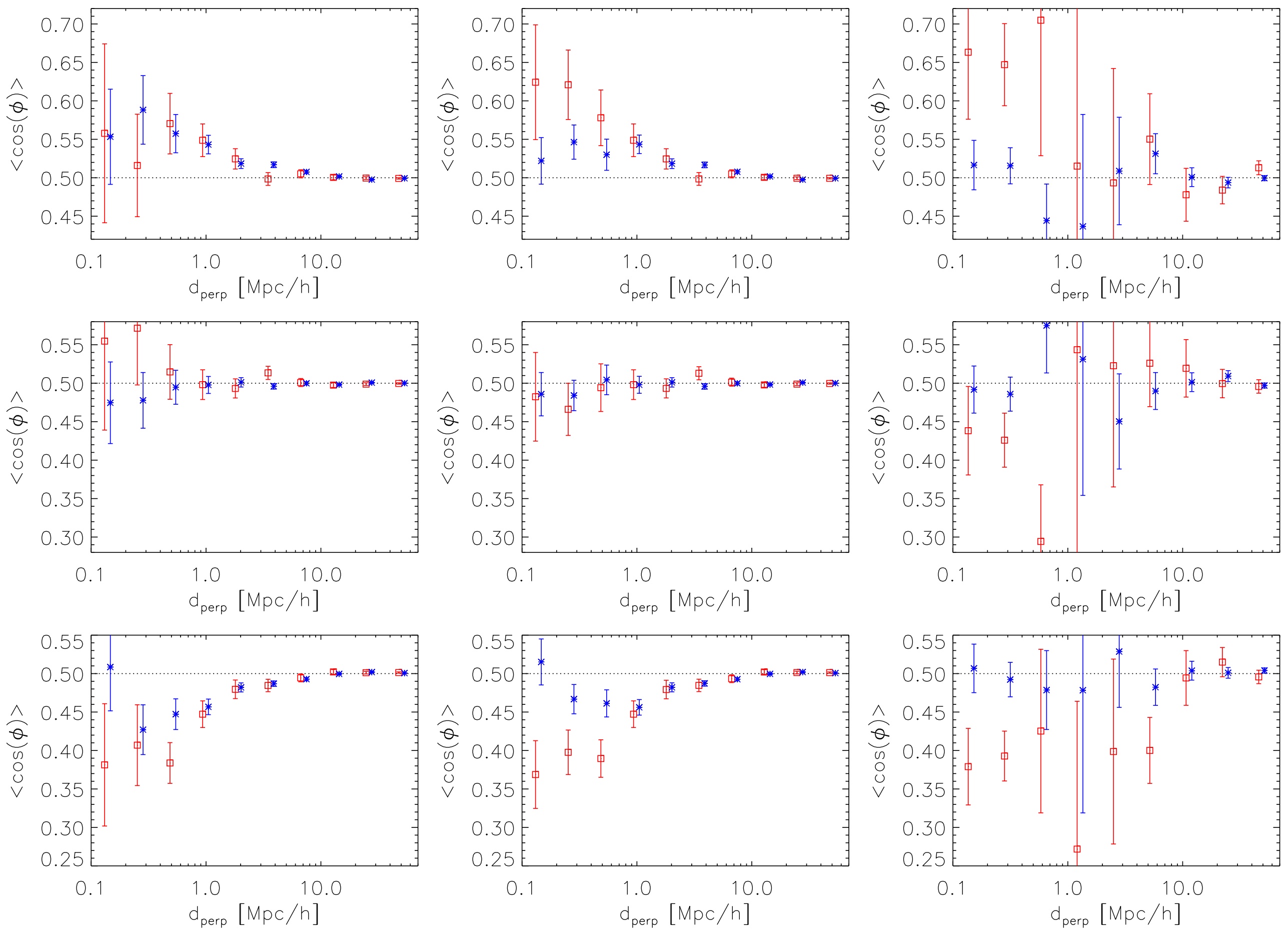

Figure 2. Alignments of the principal axes of the halos with the cluster–cluster axis as a function of perpendicular distance $d_{\rm perp}$ from that axis. The rows show the major, intermediate, and minor axes (from top to bottom). In the leftmost, center, and rightmost columns we plot alignments of halos, halos plus clusters, and only clusters, respectively. Cluster pairs which are connected by a filament are shown using squares, whereas an asterisk is used for cluster pairs for which the cluster–cluster axis cuts through a void. The dotted line shows the expectation for a random sample with no alignments.

3.3.1 Modeling the Clusters

In order to make a simple model of the tidal field, we treat the two clusters as spherical objects and we ignore the mass contained in the filaments. Given the large masses of the clusters and the relatively low average overdensity of filaments (see the discussion in Colberg et al. 2005) this simple model is reasonable.

For this dumbell–shaped configuration, use of an analytical expression for the gravitational potential is possible. We use cylindrical coordinates (ρ, θ, z) and take one of the clusters to lie at the origin with the other one on the z–axis. The gravitational potential Φ then becomes

$$\Phi = \frac{M_1}{\sqrt{\rho^2+z^2}} + \frac{M_2}{\sqrt{\rho^2+(z-L)^2}}\,, \tag{4}$$

where L is the the length of the cluster–cluster axis, and the masses of the two clusters are given by M_1 and M_2. The components of the tidal field tensor T can be computed through

$$T_{ij} = \frac{\partial^2\Phi}{\partial x_i \partial x_j}\,. \tag{5}$$

Since we are only interested in the absolute magnitude of the tidal field components we neglect the sign, thus taking the absolute value to be a measure of the stretching a body would feel.

In this axially symmetric model, there are two components of T_{ij} that stretch a spherical mass into an ellipse. They are

$$T_{zz} \;=\; \frac{M_2[2(L-z)^2-\rho^2]}{[\rho^2+(L-z)^2]^{5/2}} - \frac{M_1(\rho^2-2z^2)}{(\rho^2+z^2)^{5/2}} \tag{6}$$

and

$$T_{\rho\rho} \;=\; \frac{M_1(2\rho^2-z^2)}{(\rho^2+z^2)^{5/2}} - \frac{M_2[(L-z)^2-2\rho^2]}{[\rho^2+(L-z)^2]^{5/2}} \tag{7}$$

T_{zz} stretches along the cluster–cluster axis, whereas $T_{\rho\rho}$ stretches perpendicular to the cluster–cluster axis.

We normalize the tidal field components by dividing them by the strength of the tidal field of a Milky–Way size halo with $M_{\rm MW} = 2.5\cdot 10^{12}\,h^{-1}\,M_\odot$ at a radius of $1\,h^{-1}\,$Mpc. We use a procedure similar to the one previ-

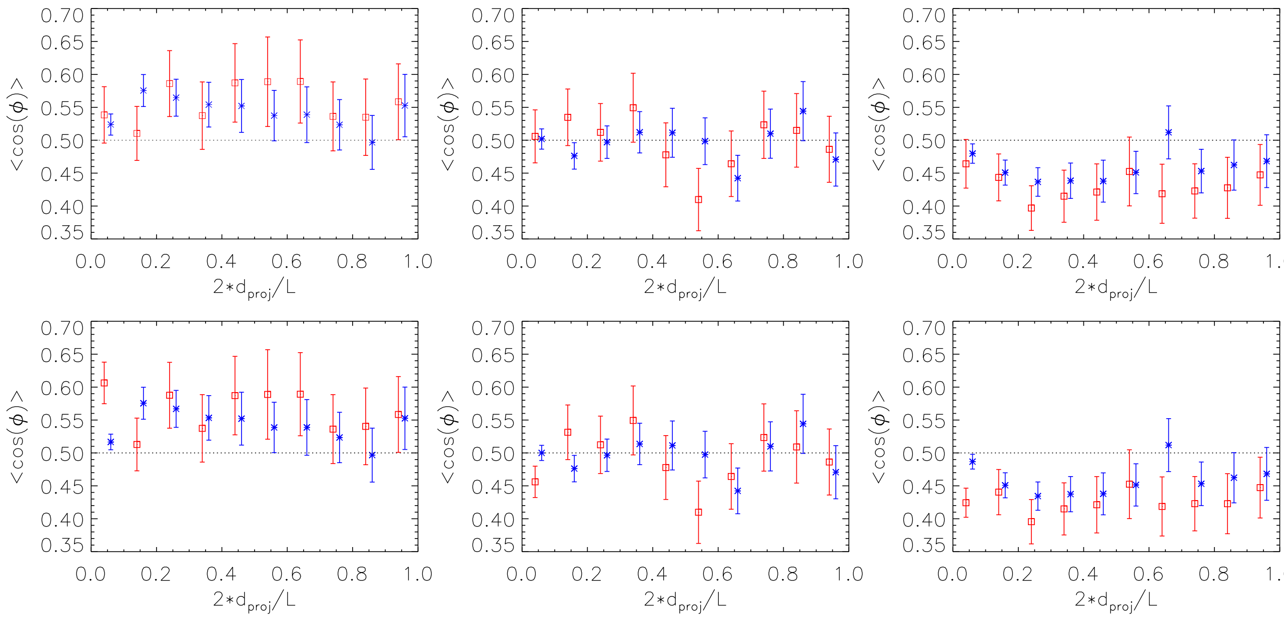

Figure 3. Alignments for the major (leftmost column), intermediate (middle column), and minor (rightmost column) halo axes, both for halos (top row) and for halos plus clusters (bottom row). The symbols are the same as in Figure 2. See main body for an explanation of the horizontal axis of each plot. The dotted line shows the expectation for a random sample with no alignments.

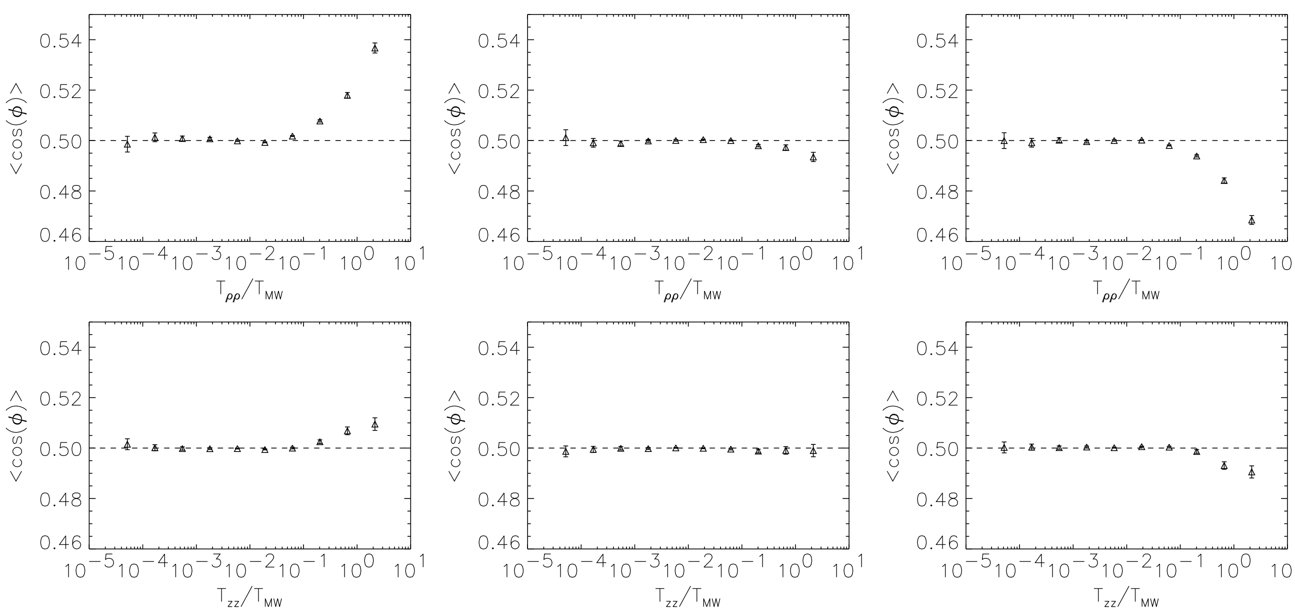

Figure 4. Alignments for the major (leftmost column), intermediate (middle column), and minor (rightmost column) halo axes as a function of local tidal fields, with stretching perpendicular to the cluster–cluster axis (top row), and parallel to the cluster–cluster axis (bottom row). The dotted line shows the expectation for a random sample with no alignments. The suffix ”‘MW”’ refers to the re–scaling of the tidal field using that of Milky Way sized halo at distance of 1 h^{-1} Mpc.

ously outlined to compute the alignments, as follows. To study $T_{\rho\rho}$, we take $\hat{\mathbf{u}}_1$ to be perpendicular to the cluster–cluster axis and pointing towards the halo and $\hat{\mathbf{u}}_2$ along one of the principal axes of the halo as before.

3.3.2 Alignments in the Tidal Field

Figure 4 shows the alignments for the two tidal–field components T_{zz} and $T_{\rho\rho}$. As before, the leftmost, center, and rightmost columns show the major, intermediate, and mi-

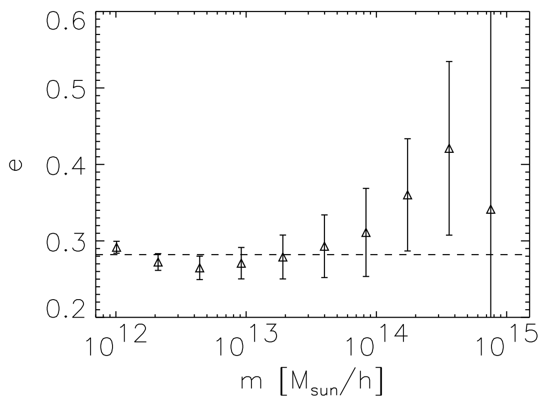

Figure 5. Halo and cluster ellipticities as a function of mass. The dotted line is the random expectation of the ellipticity.

nor halo axes, respectively. The two rows give the alignments along T_{zz} and $T_{\rho\rho}$. In each plot, the dotted line shows the expectation for a random sample with no alignments.

The stretching perpendicular to the cluster–cluster axis is about twice that parallel to the cluster–cluster axis. We note that for this analysis we do not differentiate between cluster pairs with filaments or voids in between. This also results in smaller error bars, since the sample sizes are bigger. The magnitude of this effect is smaller than alignments discussed in the previous sections. However, unlike the alignment as a function of distance from the cluster-cluster axis, the alignment with the tidal field is a much more abrupt function of tidal field strength. From Figure 4 we can see that when the tidal field is less than $\sim$ 10% of the MW field the results are statistically consistent with no alignment. The sudden change for larger values of the tidal field indicates the direct role that tidal distortions must play in aligning halos.

4 HALO AND CLUSTER ELLIPTICITIES

In the light of the results obtained so far, in particular the alignment signals and their dependence on the distance from cluster–cluster axes, it is worthile to examine ellipticities of the halos.

4.1 Ellipticity as a Function of Mass

Figure 5 shows the ellipticities of the halos and clusters in our sample as a function of their mass. The error bars assume Poissonian distributions. There is a trend for more massive clusters to be more elliptical than smaller halos, although the sample size is small. This finding agrees with the results obtained by e.g. Warren et al. 1992.

4.2 Ellipticity as a Function of Distance from Cluster–Cluster Axes

Figure 2 shows that the alignment of halos with a cluster–cluster axis depends on the distance from that axis. It is thus interesting to see whether the ellipticities are correlated with that distance as well.

Figure 6 shows halo and cluster ellipticities as a function of the distance from cluster–cluster axes. Shown are all halos (left column), all halos plus the clusters (center column), and only the 170 clusters (right column). Square and asterisk symbols denote groups associated with cluster pairs conncected by a filament or with a void in between them, respectively.

From the figure we see that within the errors there is no correlation between the ellipticities and the distance of the galaxy halos from from the cluster–cluster axes. If tidal forces are responsible for the alignments, they do not cause a difference in the overall shape of halos.

Furthermore, we also find that there is no difference between halos lying along the axes of cluster pairs connected by a filament and those cluster pairs which have a void in between them.

5 SUMMARY AND DISCUSSION

Many studies of the alignments of galaxy clusters have been carried out both with observational data (Binggeli 1982, Struble & Peebles 1985, Flin 1987, Rhee & Katgert 1987, Ulmer et al. 1989, West 1989, Rhee et al. 1992, Plionis 1994, West et al. 1995, Chambers et al. 2000 and 2002) and theoretically (Splinter et al. 1997, Onuora & Thomas 2000, Faltenbacher et al. 2002, Kasun & Evrard 2004, Hopkins et al. 2005, Basilakos et al. 2005). Most observations and all theoretical studies indicate that neighbouring galaxy clusters indeed appear to be aligned, with some uncertainties due to the facts that shapes of clusters are notoriously hard to measure observationally, and that the simulations used for the theoretical studies follow the evolution of the dark matter, which may or may not trace the distribution of the galaxies used to define observational cluster shapes.

The causes of such an alignment are not clear. Both infall of material (Van Haarlem & Van de Weygaert 1993) and tidal fields (Bond et al. 1996; also see Lee et al. 2005a, 2005b) have been suggested as explanations.

As shown in Colberg et al. (1999), the formation of clusters happens along filaments (also compare the recent direct observations of this process for the $z = 0.83$ cluster CLJ0152.7–1357 in Maughan et al. 2005 and Tanaka et al. 2005). If the infall of material causes alignments of clusters, then the presence of filaments is a prerequisite for alignments to exist. We have investigated this scenario by studying the alignments of neighbouring clusters, separating cluster pairs into those that are connected by a filament and those that are not. For this study, we have made use of the filaments identified in Colberg et al. (2005). As the rightmost column of Figure 2 shows, there is a clear difference between the two cases. Clusters connected by a filament are clearly aligned, whereas unconnected ones are not. On the basis of this result it appears the Binggeli effect can be explained by the presence of filaments, along which material falls into the clusters.

Note that this result provides another indicator of the likely presence of filaments. As Colberg et al. (2005) indicated, close pairs of clusters are candidates for the presence of a filament in between them. The presence of alignment of

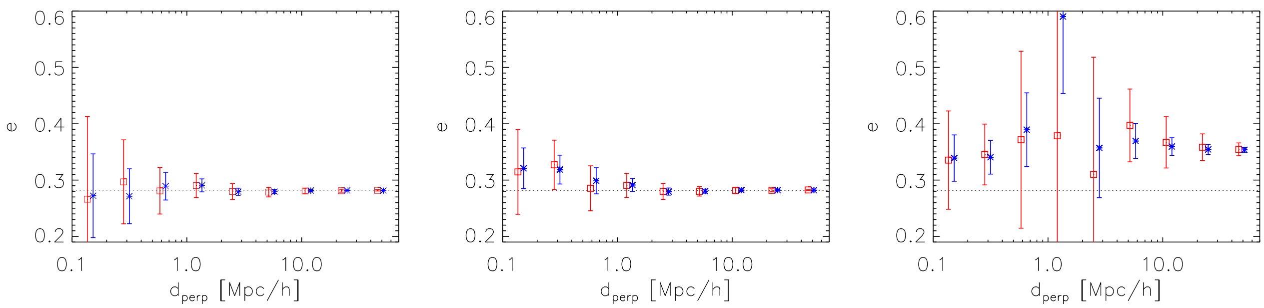

Figure 6. Halo and cluster ellipticities as a function of the distance from cluster–cluster axes. Shown are all halos (left column), all halos and clusters (middle column), and only the 170 clusters (right column). Square and asterisk symbols denote groups associated with cluster pairs conncected by a filament or with a void in between them, respectively. The dotted line is the random expectation.

the clusters adds another strong indicator. However, given the difficulties involved when measuring cluster shapes, this theoretical prediction might not be much help in practice.

It must be stressed that the presence of filaments does not mean that tidal fields play no role whatsoever in the process of aligning the halos of galaxy clusters or of galaxies themselves. As can be seen from the leftmost column of Figure 2, while filaments cause alignments of cluster–size halos, they have no discernible influence on smaller halos. An alternative way to phrase this result is to say that halos of galaxies being aligned has nothing to do with whether those halos are embedded in a filament or not. There also is no dependence of the alignments of galaxy size halos on their distance from the nearest cluster, as shown in Figure 3.

A somewhat esoteric question which one can ask is whether the strong alignments of halos seen in simulations by e.g. Heavens et al (2000), Croft & Metzler (2000) are due to halos being formed largely in filaments and being aligned with the filament direction. In this case one would expect halos to be aligned with each other as a result. In this study, we have found, however that halos are aligned with each other whether they fall in a filament or not, so that this explanation is not valid. The tidal field around each galaxy sized halo has a much more direct impact on the alignments of the halos.

We have investigated the contribution of tidal fields by modeling the tidal field of a pair of clusters analytically as a simple model of two spherical masses. Figure 4 shows the alignments for the two tidal–field components T_{zz} and $T_{\rho\rho}$. The stretching perpendicular to the cluster–cluster axis is about twice that parallel to the cluster–cluster axis. The magnitude of this effect is smaller than that of the alignment through filaments discussed above, but the abruptness of the increase in alignment signal once tidal fields become substantial leads one to the conclusion that tidal fields have a very direct influence on halo alignments.

In the light of the theoretical model of Lee et al. (2005a, 2005b), it is interesting to study whether there exists a correlation of the magnitudes of the ellipticities of halos with large-scale structure. As we have already seen, the orientiations of the ellipticities are clearly influenced by tidal fields. Figure 6 shows halo and cluster ellipticities as a function of the distance from cluster–cluster axes. There is no correlation between the ellipticities and the distance of the halos from the cluster–cluster axes, whether filament or void. Furthermore, there is no difference between cluster pairs connected by a filament and those which have a void in between them.

We are thus left to conclude that while the alignment of clusters is dominated by the infall of matter along filaments, for the vast majority of halos only tidal fields determine alignments of halos. As an aside, we note that this implies that Pimbblet (2005)'s filament finding mechanism which is based on using alignments to find filaments is unlikely to be successful. This judgment is however based on the assumption that the stellar parts of galaxies will align in a similar way to the dark matter, something which must be tested.

ACKNOWLEDGMENTS

This project is supported by the National Science Foundation, NSF AST-0205978.

The simulation discussed here was carried out as part of the Virgo Consortium programme, on the Cray T3D/Es at the Rechenzentrum of the Max–Planck-Gesellschaft in Garching, Germany, and at the Edinburgh Parallel Computing Center. We are indebted to the Virgo Consortium for allowing us to use it for this work.

REFERENCES

Agustsson, I, & Brainerd, T., 2005, ApJ submitted, astro-ph/0509405

Allgood B., Flores R.A., Primack J.R., Kravtsov A.V., Wechsler R.H., Faltenbacher A., Bullock J.S., astro-ph/0508497

Bailin J., Steinmetz M., 2004, ApJ, 616, 27

Basilakos S., Plionis M., Yepes G., Gottlöber S., Turchanino V., astro-ph/0505620

Binggeli B., 1982, A&A, 107, 338

Bond J.R., Kofman L., Pogosyan D., 1996, Nature, 380, 603

Chambers S.W., Melott A.L., Miller C.J., 2000, ApJ, 544, 104

Chambers S.W., Melott A.L., Miller C.J., 2002, ApJ, 565, 849

Colberg J.M., White S.D.M., Jenkins A., Pearce F.R., 1999, MNRAS, 308, 593
Colberg J.M., Krughoff K.S., Connolly A.J., 2005, MNRAS, 359, 272
Croft, R.A.C., & Metzler C., 2000, ApJ, 545, 561
Colless M. et al. (2dF Collaboration), 2001, MNRAS, 328, 1039
Faltenbacher A., Gottlöber S., Kerscher M., Müller V., 2002, A&A, 395, 1
Flin P., 1987, MNRAS, 228, 941
Heavens, A., Refregier, A., Heymans, C., 2000, MNRAS, 319, 649
Hopkins P.F., Bahcall N.A., Bode P., 2005, ApJ, 618, 1
Jenkins A. et al. (Virgo Consortium), 1998, ApJ, 499, 20
Jing Y.P., Suto Y., 2002, ApJ, 574, 538
Kasun S.F., Evrard A.E., 2005, ApJ, 629, 781
Lee J., Kang X., Jing Y.P., 2005a, ApJ, 629, 5
Lee J., Jing Y.P., Suto Y., 2005b, ApJ, 632, 706
Li, S.F., & Croft, R.A.C, 2005, MNRAS, *submitted*.
Mandelbaum, R., Hirata, C.M., Ishak, M., Seljak, U., & Brinkmann, J., 2005, MNRAS submitted, astro-ph/0509026
Maughan B.J., Ellis S.C., Jones L.R., Mason K.O., Cordova F.A., Priedhorsky W., accepted for publication in ApJ, astro–ph/0511466
Moore B., Quinn T., Governato F., Stadel J., Lake G., 1999, MNRAS, 310, 1147
Navarro J.F., Frenk C.S., White S.D.M., 1997, ApJ, 490, 493
Onuora L.I., Thomas P.A., 2000, MNRAS, 319, 614
Paz D.J., Lambas D.G., Padilla N., Merchan M., astro-ph/0509062
Pimbblet K.A., 2005, MNRAS, 358, 256
Plionis M., 1994, ApJ, 95, 401
Plionis M., Basilikos S., 2002, MNRAS, 329, L47
Rhee G.F.R., Katgert P., 1987, A&A, 183, 217
Rhee G.F.R., Van Harleem M., Katgert P., 1992, AJ, 103, 1721
Seljak U. et al., 2005, PhRvD, 71, 10, 103515
Spergel D.N. et al., 2003, ApJS, 148, 175
Splinter R.J., Melott A.L., Linn A.M., Buck C., Tinker J., 1997, ApJ, 479, 632
Springel V. et al. (Virgo Consortium), 2005, Nature, 435, 629
Struble M.F., Peebles P.J.E., 1985, AJ, 90, 582
Tanaka M., Kodama T., Arimoto N., Tanaka I., astro–ph/0511296
Ulmer M.P., McMillan S.L.W., Kowalski M.P., 1989, ApJ, 338, 711
Van Haarlem M., Van de Weygaert R., 1993, 1993, ApJ, 418, 544
Warren, M.S., Quinn, P.J., Salmon, J.K., & Zurek, W., 1992, ApJ, 399, 405
West M.J., 1989, ApJ, 347, 610
West M.J., Jones C., Forman W., 1995, ApJ, 451, L5
York D.G. et al. (SDSS Collaboration), 2000, AJ, 120, 1579